Revista GEOCIÊNCIAS

unesp

ISSN: 1980-900X (online)

BOAT-GENERATED WAVES AND EROSION ON THE SHORE OF THE XINGÓ POWER PLANT RESERVOIR

ONDAS GERADAS POR BARCO E EROSÃO NAS MARGENS DO RESERVATÓRIO DA USINA HIDRELÉTRICA DE XINGÓ

Francisco Sandro Rodrigues HOLANDA[1], Lilian de Lins WANDERLEY[2], Luiz Diego Vidal SANTOS[3], Igor Pinheiro da ROCHA[4], Mairon Vinícius Sousa OLIVEIRA[5], Alceu PEDROTTI[4]

[1]Universidade Federal de Sergipe. Av. Marechal Rondon, s/n - Jardim Rosa Elze, São Cristóvão – SE. E-mail: fholanda@infonet.com.br

[2]Universidade Federal de Sergipe. Programa de Pós-Graduação em Geografia. E-mail: lilianwanderley@uol.com.br

[3]Universidade Federal de Sergipe - Departamento de Engenharia Agronômica. Programa de Pós-Graduação em Ciências da Propriedade Intelectual. E-mail: vidal.center@academico.ufs.br

[4]Universidade Federal de Sergipe / Laboratório de Erosão e Sedimentação LABES. E-mail: igor@iande.eng.br

[5]Universidade Federal de Sergipe - Departamento de Engenharia Agronômica. Graduação em Engenharia Agronômica. E-mail: mairon0014@gmail.com

ABSTRACT - In fluvial environments, factors such as longitudinal slope, water volume, channel shape (cross section), bed roughness, and water viscosity affect water speed in different sections of the channel. Boats in these environments introduce an additional factor by generating primary and secondary wave systems. The objective of this work was to describe the erosive effects of waves from tour boats on the banks of the reservoir at the Xingó hydroelectric power plant in northeastern Brazil. Reservoir data were gathered through onsite measurements as well as environmental monitoring systems, while wave heights were calculated according to the effects of transverse and divergent waves. The wave propagation behavior observed in this present study alone cannot be responsible for erosion on the banks and slopes of the lake, since this is also associated with the presence of wind fetch, human activities, deposit of transported sediments resulting from operations at the power plant, as well as other factors. The findings corroborated observations that the tour boats do not directly cause erosion, since they are limited to subcritical speeds, but wind was seen to be directly related to this phenomenon.
Keywords: Wind. Froude number. São Francisco River.

RESUMO - Em ambientes fluviais, fatores como inclinação longitudinal, volume de água, formato do canal (seção transversal), rugosidade do leito e viscosidade da água afetam a velocidade da água em diferentes seções do canal. Os barcos nesses ambientes introduzem um fator adicional ao gerar sistemas de ondas primárias e secundárias. O objetivo deste trabalho foi descrever os efeitos erosivos das ondas dos barcos de turismo nas margens do reservatório da Usina Hidrelétrica de Xingó, no nordeste do Brasil. Os dados dos reservatórios foram coletados por meio de medições no local e também por sistemas de monitoramento ambiental, enquanto as alturas das ondas foram calculadas de acordo com os efeitos das ondas transversais e divergentes. O comportamento de propagação das ondas observado no presente estudo por si só não pode ser responsável pela erosão nas margens e encostas do lago, pois também está associada à presença de *wind fetch*, atividades antrópicas, depósito de sedimentos transportados decorrentes de operações na usina, bem como outros fatores. Os achados corroboram as observações de que os barcos de passeio não causam erosão diretamente, pois se limitam a velocidades subcríticas, mas o vento mostrou estar diretamente relacionado a esse fenômeno.
Palavras-chave: Vento. Número de Froude. Rio São Francisco.

INTRODUCTION

Boat-generated waves, sediment transport and erosion on the banks of rivers and lakes can alter vegetation as well as the fluid dynamics and geological structure of water bodies (Miranda et al., 2020).

Waves are important sources of kinetic energy. Known as "energy in transition" because they involve mechanical loads with significant power and constant movement, their impact can cause mechanical damage to fixed objects (Baumann et al., 2017; Liu et al., 2017).

Some ocean waves are currently being explored for electricity generation (Plamer et al., 2017). Jahangir & Mazinani (2020) demonstrated that waves in the southern Caspian Sea could potentially generate 3.5Kw per meter over a 15-year period, indicating major potential.

Waves are mostly a result of wind, and are often accentuated as they move across long distances and open waters and propagate on the surface.

In general, winds blow consistently over large portions of confined water and their energy is transported to the shore of lakes and dams as waves (Ozkan et al., 2020).

When waves propagate toward the coast, their height increases as a result of several hydrodynamic processes close to the shore, including wave capture and refraction (Bittencourt et al., 2007; Netto et al., 2019), wave breaking (Lara et al., 2006; Pizzo et al., 2018), and reflection and diffraction (Zhu et al., 2020).

The same kinetic energy resulting from waves contributes to sediment transport and erosion by resuspending sediments resulting from solitary or grouped waves (Boegman & Stastna, 2019; Illig & Bachèlery, 2019), shear induced by waves and currents in lakes, as well as particle movement (Forgia et al., 2020) and marsh edge retreat from wave erosion (Elsey-Quirk et al., 2019).

In fluvial environments, water speed depends on important factors such as longitudinal slope, water volume, channel shape (cross section), bed roughness, and water viscosity, all of which affect speed in different sections of the channel in which it flows.

Any obstacle negatively influences flow efficiency, and consequently water speed and flow (turbulent or laminar) are related to the fluvial current, which transports the sedimentary load in various manners (suspension, jumping and rolling) according to particle size and shape and current characteristics; all these variables influence river relief morphology (Carvalho, 2009; Dai Prá et al., 2016; Grzegorczyk et al., 2019). Boats can also cause agitation in bodies of water (Pereira et al., 2016).

Environmental balance depends on cyclical arrangements and is susceptible to human actions including sustainable management of water systems (Teixeira, 2016).

In Brazil, these systems are not only relevant in supplying water for human use, but also provide navigation routes as cargo transport and tourism increase on narrow waterways that may include confined portions (Paula et al., 2019).

These activities have caused damage including reduced numbers of riparian plant species that are sensitive to water movement, remobilization of sediments in shallow portions, emission of effluents from passenger craft, and river and lake bank erosion caused by cargo boats (Holanda et al., 2020; Rapaglia et al., 2015).

Regular boat and cargo traffic is steadily increasing in major waterways such as those in the Amazon Region, where cargo shipments increased 9.75% between 2018 and 2019, from 22,289,925 to 24,462,315 tons (ANTAQ, 2020).

The Institute of Strategic Social and Environmental Intelligence of the Amazon (PIATAM) has developed plans to reduce the risks of accidents that could generate environmental impacts on river areas (Piatam, 2020).

Nevertheless, even with government efforts to study and prevent impacts on waterways, few studies have addressed river or lake bank erosion resulting from boats.

Boat-generated waves have a complex distribution, forming primary (first order) and secondary (second order) wave systems (Bittencourt et al., 2007; Themistocles, 2016).

A primary wave system consists of a frontal wave and a sharp depression in water level associated with a "return" moving in the opposite direction of the boat.

The end of this depression contains a stern wave, which is relatively high and has a shorter period (Gomes, 2014). This type of wave is also known as a compressive wave and is propagated from uniaxial deformations generated by boats (Assumpção & Neto, 2000; Nascimento, 2019).

Secondary waves, which have a shorter period, are most common and have been the subject of various studies because of the damage they cause; these systems are composed of transverse and divergent waves that interact and may cause significant bank damage.

Divergent waves spread equally on both sides of the boat if it does not change direction, as well as to the front of the bow or front of the ship, while transverse waves move toward the stern (Gomes, 2014).

Both boat speed and secondary nonlinear wave forces can amplify waves and their induced responses (Kong et al., 2017). Furthermore, boat movement can be defined based on speed into displacement, semi-sliding, or sliding (Pessin, 2017).

The objective of this article is to describe the erosive effects of waves from tour boats on the reservoir banks at the Xingó hydroelectric power plant in northeastern Brazil.

MATERIAL AND METHODS

The experimental site, the reservoir of the Xingó hydroelectric power station, is located in the state

of Sergipe, Brazil, near the border with Alagoas (9°37'25"S 37°47'54"W); the plant is 12 kilometers from Piranhas, Alagoas and 6 kilometers from the central region of the municipality of Canindé de São Francisco. The power station is in the lower course of the São Francisco River Basin, within the channel of the São Francisco River approximately 65 km downstream from the Paulo Afonso hydroelectric plant complex (in the state of Bahia). The reservoir is an important tourist attraction, and has also been used to irrigate crops and supply water to the local population. The climate is defined as semi-arid megatherm, with average annual temperature of 25.3°C and rainy period from March to July with average annual rainfall of 521 mm (INMET, 2020); shrubby hyper-xerophilous Caatinga vegetation is present. The lake has a surface of 908.2 km²; catamaran berths are found on both banks, mainly in Canindé de São Francisco (Holanda et al., 2020), (Figure 1), and smaller boats provide the essential tourism infrastructure for the Xingó area.

Figure 1 - Xingó Reservoir, along the São Francisco River. Source: Adapted from Google Earth.

Data collection

A topobathymetric survey of the points of interest in the Xingó reservoir was conducted using acoustic doppler current profile (ADCP, Rio Grande Model) for bathymetry and global positioning system technology (GPS) to determine the position of the equipment; ADCP provided measurements of the lake (propagation time) as well as the relative speed of the boat in relation to the fixed bottom (Doppler effect) and the relative speed of particles suspended in the water, which is the speed of the liquid mass (also determined by the Doppler effect). The orientation was determined using an electronic compass.

The primary and secondary waves were initially classified and quantified using the boat speed. Because speed is directly related to the water agitation caused by the tour boats, a maximum speed limit is defined for boats to avoid erosion on lake banks (Gomes, 2014). In our study, the speed limit was obtained using Equation 1:

$$V_L = (gh)^{1/2} \quad (1)$$

Where:

V_L represents the speed limit (m/s)

g is the acceleration of gravity (m/s^2), and

h is the water depth (m)

The speed limit was obtained in greater detail, considering the morphometry of the boats, using Equation 2.

$$V_L = (gL/2\pi)^{1/2} \quad (2)$$

The speed limit calculations exclusively considered the catamaran-type tour boats that regularly navigate the Xingó reservoir on a regular route. These boats were divided into two groups according to hull width (group 1: width <8 m and group 2: width ≥8 m, respectively); examples of boats in each group are shown in figure 2.

The intersection between the secondary waves generates a line where the tallest waves are located, known as the cusp line. The angle formed by this cusp line mainly depends on the Froude number (Fr) of the flow, which is used to determine how boat motion will affect wave formation (Liang & Chen, 2017).

The Froude number is related to different parameters such as water depth (Canellas et al., 2016) or boat length; when the channel depth provides a limitation, it is represented by Fr_h and is calculated using Equation 3.

$$Frh = \frac{V}{(g\ h)^{\frac{1}{2}}} \qquad (3)$$

Where:
V represents the boat's working speed (m/s)
h is channel depth (m), and
g represents acceleration of gravity (m/s^2).

Several speed variation intervals could be defined according to the Froude number; because Frh was below 0.75 for all boats, according to Macfarlane et al. (2014) speed was considered subcritical.

Figure 2 - Tour boats: representative of group 1 (*Delmiro Gouveia*) at left, representative of group 2 (*Frei Damião*) at right.

By definition, lakes are confined waters which are relatively calm and deep. In deep waters, the wedge formed under the conditions established by Macfarlane et al. (2014) at a 19.28° angle to the boat's navigation line. In these deeper water conditions, the Froude number was defined according to boat length (L) and calculated using Equation 4.

$$FrL = \frac{V}{(g\ L)^{\frac{1}{2}}} \qquad (4)$$

Where:
V represents the boat's working speed (m/s)
g acceleration of gravity ($m/s2$), and
L the length of the boat (m)

Consequently, in deep water the Froude number calculated according to boat length provided a better description of the waves generated, and classified boat motion (which in turn depends on speed) into three categories: displacement, semi-slip, and slip. Each of these movements is associated with a certain range of values for Fr_L and Fr_∇, where Fr_∇ represents the Froude number relative to the volume of water displaced by the boat's passage. According to Archimedes' principle, this corresponds to the volume of the submerged hull, calculated using Equation 5 and Equation 6.

$$FrL = \frac{V}{(g\ \nabla)^{\frac{1}{2}}} \qquad (5)$$

Where:
V represents the boat's working speed (m/s)
g acceleration of gravity ($m/s2$), and
∇ displaced water volume (m)

$$\nabla = \frac{1}{2}(\pi * r2 * L) \qquad (6)$$

Where:
Π = 3.1416
r = radius, and
L = boat length

Wave height calculation - Hochstein Method

Wave height was calculated using the cross-sectional area of the channel and the submerged transverse area of the boat, as well as the length of the boat in movement, according to Equation 7.

$$Hi = 0.0448\ V^2 \left(\frac{D}{L}\right)^{0.5} \left(1 - \frac{BD}{Ac}\right)^{-2.5} \qquad (7)$$

Where:
Hi is the height of the interference wave
V represents the boat's working speed *(m/s)*
D represents the draft
L the length of the boat
B the width of the boat, and
A_c the area of the channel section at the midpoint

of the boat.

To calculate A_c (the area of the channel section at the midpoint of the boat), the channel section, depth, and boat width were considered.

RESULTS AND DISCUSSION

It is important to examine the tour routes to understand how waves form. Figure 3 shows the regular route for all the tour boats listed in table 1; there are only slight variations in the places where these boats dock to load and unload cargo and passengers.

The same figure also shows a longitudinal profile of the lake's depth between the starting and ending points of the usual tour route, showing that channel depth varied between 10 and 125 m.

In order to better understand the waves formed by the boats, the speed limit calculated by V_L (Equation 1) is shown in table 2. The speed limit is an equipment-dependent recommendation to avoid lake shore erosion based on the values presented, and is consequently important for passenger safety as well as to protect the local environment. This parameter differs from working speed, since it considers the acceleration of the boat as well as its length. Only the *Delmiro Gouveia* (group 1) had unique V_L values, which are probably explained by its shorter length. Note that the boats described in table 2 represent the craft used in this area in terms of size, frequency of operations throughout the year, as well as regular function in the routes they offer tourists.

Table 1 - Technical specifications of boats providing sightseeing tours of the Xingó reservoir.

Boat Name	Maximum Capacity (Units)	Boat Working Speed (m/s)/(km/h)	Length (m)	Width (m)	Average Draft (m)	Hull Height (m)
Delmiro Gouveia	189	4.47/16.09	19.00	7.50	0.90	2.10
Rei do Cangaço	250	4.02/14.47	20.00	8.0	1.0	2.50
Padre Cicero	250	4.02/14.47	20.00	8.0	1.0	2.50
Luiz Gonzaga	250	4.02/14.47	20.00	8.0	1.0	2.50
Frei Damião	250	4.02/14.47	20.00	8.0	1.0	2 .50
Patativa do Assaré	250	4.02/14.47	20.00	8.0	1.0	2.50
Apolônio Sales	250	4.91/17.67	20.00	8.0	1.0	2.50

Source: ATOLX - Lake Operators Association of the Xingó Power Plant

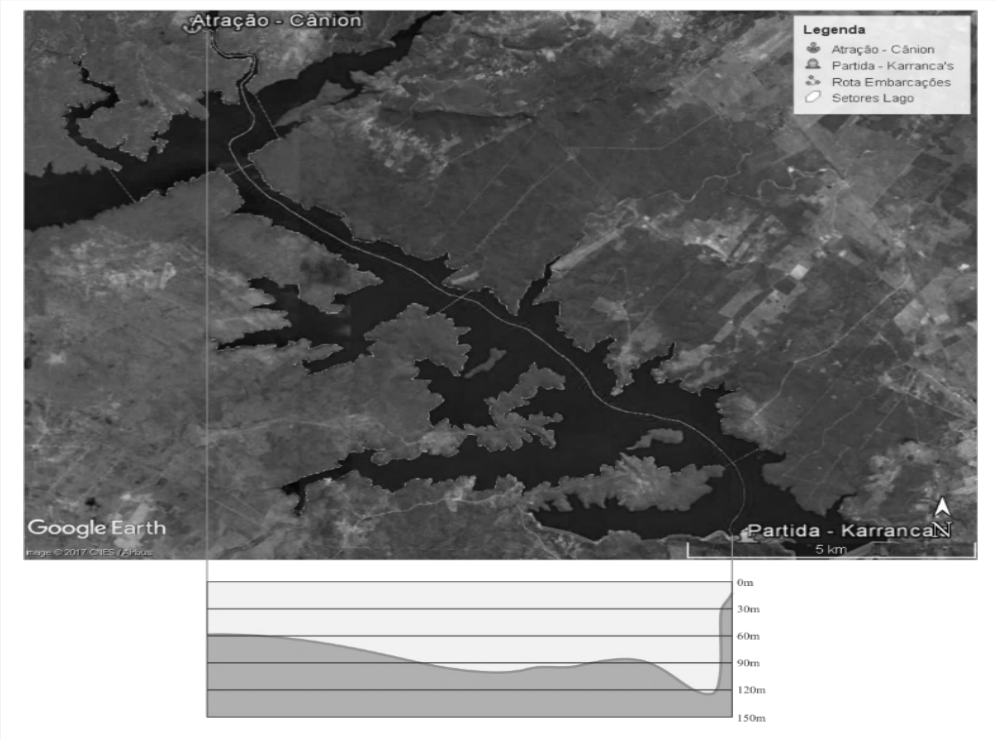

Figure 3 - Top: longitudinal profile of the boat route; starting point at bottom (Karranca) and endpoint at top (canyon). Bottom: submerged profile of the boat route. Source: The authors, adapted from Google Earth

Table 2 - Working speed and speed limit (V_L).

Boat (name)	Length (m)	Working Speed (m/s) / (km/h)	V_L (m/s) / (Km/h)
Delmiro Gouveia	19.00	4.47/16.09	29.60/61.56
Rei do Cangaço	20.00	4.02/14.47	29.60/63.03
Padre Cicero	20.00	4.02/14.47	29.60/63.03
Luiz Gonzaga	20.00	4.02/14.47	29.60/63.03
Frei Damião	20.00	4.02/14.47	29.60/63.03
Patativa do Assaré	20.00	4.02/14.47	29.60/63.03
Apolônio Sales	20.00	4.91/17.67	29.60/63.03

The speed limit is an equipment-dependent recommendation to avoid lake shore erosion based on the presented values. This information is very important for passenger safety as well as to protect the local environment. The waves generated by the boats are directly dependent on the Froude number of the flow, which indicates the intersection between the secondary waves where a line with the tallest waves is located (the cusp line), making it possible to predict how the boat will propagate waves. Table 3 shows the Froude number (Frh) of the waves generated by the boats, which differs between the two groups.

At subcritical speeds, divergent waves have small crests, and the Kelvin wedge (cusp lines) is at a 19.28° angle, as shown in figure 4.

The values calculated for Fr_L and Fr_∇ are shown in Table 4, and are less than 0.4 and 1.3, respectively, which defined the boat movement as displacement; FrL and $Fr\nabla$ values of 0.4 a 0.9 and 1.0 a 3.0 or > 0.9 and > 2.3 characterize movement as semi-slip and slip, respectively (Gomes, 2014), unlike the values for the boats in this study.

Table 3 - Froude number values (Frh) for the waves generated by the tour boats in the Xingó power plant reservoir.

Boat	Working speed (m/s) / (km/h)	Froude number (calculated) (Fr_h)
Delmiro Gouveia	4.47/16.09	0.15
Rei do Cangaço	4.02/14.47	0.13
Padre Cicero	4.02/14.47	0.13
Luiz Gonzaga	4.02/14.47	0.13
Frei Damião	4.02/14.47	0.13
Patativa do Assaré	4.02/14.47	0.13
Apolônio Sales	4.91/17.67	0.16

Figure 4 - Development of divergent waves with Kelvin wedge at a 19.28° angle to the direction of travel.

Table 4 - Froude number values derived from boat length (L) and volume of the submerged hull (∇) (FrL and $Fr\nabla$, respectively) for the waves generated by the boats.

Boat	Working speed (m/s)	Boat length (m)	Froude number (Fr_L)	Froude number (Fr_∇)
Delmiro Gouveia	4.47	19	0.32	0.36
Rei do Cangaço	4.02	20	0.28	0.32
Padre Cicero	4.02	20	0.28	0.32
Luiz Gonzaga	4.02	20	0.28	0.32
Frei Damião	4.02	20	0.28	0.32
Patativa do Assaré	4.02	20	0.28	0.32
Apolônio Sales	4.91	20	0.35	0.39

In displacement-type movement, the weight of the boat is supported only by the thrust of water over it; the bow is directed downward, and the relatively low speed causes small waves (Bispo, 2007), in agreement with our findings.

In cases where boats move very close to the banks, the embankment can affect how secondary waves propagate; this was the case in the Xingó reservoir, where boat speed was considered subcritical (since values for Frh were > 0.75, as shown in table 3).

Like waves generated by wind action, the waves produced by boat movement are influenced by the dimensions of the body of water.

Some studies have developed several empirical formulations based on measurements in the laboratory and in the field that can predict wave height according to the geometry of the channel and boats (Aguiar, 2018). These formulations permit initial estimates of the waves generated by boat passage and can help determine potential erosion on the banks of the body of water.

The height of the interference wave (Hi) varied for waves generated by the boats in groups 1 and 2, as depicted in Tables 5 and 6. The wave height refers to the maximum height that occurs in the vicinity of the boat.

Table 5 presents values for Hi for the boat in group 1 in different bathymetric sections of the entire route it routinely travels, where depths vary. Note that the data generated from interference wave height also depend on the technical specifications of each boat, among other factors. Over time, interference wave height results from the sum of the effects of the transverse and divergent waves.

Table 6 presents the height data for interference waves and the boats in group 2; because of their different technical specifications, different values were seen for *Hi* even though these boats followed the same route as the boat in group 1. These values were also related to the area of each section of the channel where the midpoint of the boat passed.

Table 5 - Values related to *Hi* (interference wave height) and other variables used to calculate this parameter for the boat in group 1

ID	Section	Route depth (m)	Boat width (m)	Ac (m)	Hi (m)
1	5	132.48	7.00	918.61	0.19
2	13	86.73	7.00	598.36	0.20
3	4	94.22	7.00	650.79	0.19
4	1	111.32	7.00	770.49	0.19
5	12	98.21	7.00	678.72	0.19
6	2	74.19	7.00	510.58	0.20
7	11	61.47	7.00	421.54	0.20
8	10	56.47	7.00	385.70	0.20

Note: Group 1: *Delmiro Gouveia*. Half hull: 1.05 m.

Table 6 - Values related to *Hi* (interference wave height) and other variables used to calculate this parameter for the boats in group 2.

ID	Section	Route depth (m)	Boat width (m)	Ac (m)	Hi (m)
1	5	132.48	8.00	1049.84	0.1649
2	13	86.73	8.00	683.84	0.1669
3	4	94.22	8.00	743.76	0.1662
4	1	111.32	8.00	880.56	0.1655
5	12	98.21	8.00	775.68	0.1661
6	2	74.19	8.00	583.52	0.1675
7	11	61.47	8.00	481.76	0.1687
8	10	56.35	8.00	440.80	0.1694

Note: Group 2: *Rei Do Cangaço, Padre Cicero, Luiz Gonzaga, Frei Damião, Patativa do Assaré,* and *Apolônio Sales.* Half hull: 1.25 m.

Tables 5 and 6 show that the interference wave height values (Hi) are absolutely compatible with topobathymetric data obtained onsite via ADCP.

Observed and recorded erosive events did not appear to be directly related to boat movement;

instead, wind and wind tracks (fetch) directly affected the observed erosion sites. In an investigation of waves generated from wind tracks in the Xingó reservoir, Holanda et al. (2020) noted erosion on the bank of the lake in the same direction as the winds, which propagated waves that may vary according to soil type on the slopes (Guo et al., 2020).

Onsite observations made during data collection indicate that the wave propagation behavior described in this study is not solely responsible for erosion on the banks of the lake, since it may also be associated with wind tracks, human activities, deposit of transported sediments resulting from operations at the power plant, as well as other factors such as those indicated by Miranda et al. (2020) and Sajinkumar et al. (2020).

CONCLUSIONS

The movement of the boats in this study, which was characterized as displacement, is perfectly justified by the subcritical speed at which they traveled, and this low speed causes small waves with small crests and consequently short duration.

Because of their low energy, these waves not present any risk of erosion when the boats approach the reservoir banks as they follow their regular tour routes.

The generated waves, particularly the height of the interference wave (Hi), were seen to vary according to the dimensions of the boats. The results for interference wave height (Hi) related to the secondary wave system, which is the sum of the effects of transverse and divergent waves, were compatible with the discrete movement of water in the form of waves produced by boats.

This study establishes that the tour boats that operate in the Xingó power plant reservoir and provide income for local residents do not cause erosion on the lake banks. Future studies are needed to examine the interaction between secondary waves generated by boats and hydrological and hydrodynamic factors, sediment transport, geotechnical aspects, and anthropic activities in order to avoid erosion caused by secondary waves.

REFERENCES

AGUIAR, T.C.G.R. **Análise do comportamento dinâmico de uma embarcação de planeio via CFD**. Rio de Janeiro, 2018. Tese (Doutorado), Universidade Federal do Rio de Janeiro.

ANTAQ, A.N.T.A. **Base de Dados Estatístico Aquaviário (Anuário-2019)**. Anuário, n. 1. Brasília-DF: ANTAQ, 2020. Disp. em: http://web.antaq.gov.br/Anuario/. Acesso em: 13 fev. 2020.

ASSUMPÇÃO, M. & NETO, C. M. D. Sismicidade e estrutura interna da terra. **Decifrando a terra. São Paulo, Oficina de Textos**, São Paulo-SP, p. 43–62, 2000.

BAUMANN, J.; CHAUMILLON, E.; BERTIN, X., SCHNEIDER, J.L.; GUILLOT, B.; SCHMUTZ, M. Importance of infragravity waves for the generation of washover deposits. **Marine Geology**, v. 391, p. 20–35, 1 set. 2017.

BISPO, M.J. Impacts of boat-generated waves on macroinfauna: Towards a mechanistic understanding. **Journal of Experimental Marine Biology and Ecology**, v. 343, n. 2, p. 187–196, 2007.

BITTENCOURT, A.C.D.S.P.; DOMINGUEZ, J.M.L.; FONTES, L.C.S.; SOUSA, D L.; SILVA, I.R.; SILVA, F.R. WAVE Refraction, River Damming, and Episodes of Severe Shoreline Erosion: The São Francisco River Mouth, Northeastern Brazil. **Journal of Coastal Research**, United States, p. 930–938, 2007.

BOEGMAN, L. & STASTNA, M. Sediment Resuspension and Transport by Internal Solitary Waves. **Annual Review of Fluid Mechanics**, Stanford-EUA, v. 51, n. 1, p. 129–154, 2019.

CANELLAS, A.V.B.; DAI PRÁ, M.; MARQUES, M.G., TEIXEIRA, E.D.; MARTINEZ, C.B. Características das flutuações de pressão a jusante de dissipadores tipo concha com ângulo de 45º. **Rbrh: Revista Brasileira de Recursos Hídricos**, Porto Alegre, v. 21, n. 1, p. 134–142, 2016.

CARVALHO, T.M. Avaliação do transporte de carga sedimentar no médio rio Araguaia. **Geosul**, Santa Catarina-RS, v. 24, n. 47, p. 147–160, 2009.

DAI PRÁ, M.; PRIEBE, P. S.; SANAGIOTTO, D.G.; MARQUES, M.G. Dissipação de energia do escoamento deslizante sobre turbilhões em vertedouros em degraus de declividade 1V:1HEnergy dissipation in skimming flow at stepped spillways with 1V:1H slope. **Ingeniería del agua**, Cordoba, v. 20, n. 1, p. 1–12, 2016.

ELSEY-QUIRK, T.; MARIOTTI, G.; VALENTINE, K.; RAPER, K. Retreating marsh shoreline creates hotspots of high-marsh plant diversity. **Scientific reports**, United Kingdom - UK, v. 9, n. 1, p. 1–9, 2019.

FORGIA, G.L.A; TOKYAY, T.; ADDUCE, C.; CONSTANTINESCU, G. Bed shear stress and sediment entrainment potential for breaking of internal solitary waves. **Advances in Water Resources**, Amsterdã, v. 135, p. 103475, 1 jan. 2020.

GOMES, D.N.P.L. **Avaliação da geração de ondas por ação do vento e de embarcações em albufeiras. Estudo de caso**. Porto-PT, 2014.

GRZEGORCZYK, V.; SANTOS, M.L. DOS; PAGOTTO, D. As características sedimentares do transporte da carga de fundo nas confluências do Rio Ivinhema-MS com o Rio Paraná. **Raega-O Espaço Geográfico em Análise**, Curutíba-PR, v. 46, n. 1, p. 58–74, 2019.

GUO, B.; SUBRAHMANYAM, M.V.; LI, C. Waves on Louisiana Continental Shelf Influenced by Atmospheric Fronts. **Scientific Reports**, v. 10, n. 1, p. 1–9, 2020.

HOLANDA, F.S.R.; WANDERLEY, L.L.; MENDONÇA, B.S.; SANTOS, L.D.V.; ROCHA, I.P.; PEDROTTI, A. Formação de ondas e os processos erosivos nas margens do lago da UHE Xingó. **Revista Brasileira de Geografia Física**, v. 13, n. 2, p. 887–902, 2020.

IlLIG, S. & BACHÈLERY, M.L. Propagation of Subseasonal Equatorially-Forced Coastal Trapped Waves down to the Benguela Upwelling System. **Scientific Reports**, Alemanha, v. 9, n. 1, p. 1–10, 2019.

INMET - Instituto Nacional de Meteorologia. 2020. **INMET**. [Informacional]. Disponível em: http://www.inmet.gov.br/portal/. Acesso em: 13 fev. 2020.

JAHANGIR, M.H. & MAZINANI, M. Evaluation of the convertible offshore wave energy capacity of the southern strip of the Caspian Sea. **Renewable Energy**, Amsterdã, v. 152, p. 331–346, 2020.

KONG, X.; HE, Q; YANG, B.; HE, W., XU, F; JANSSEN, A.B.G.; KUIPER, J.J.; VAN GERVEN, L.P.A.; QIN, N.,; JIANG, Y.; LIU, W.; YANG, C.; BAI, Z.; ZHANG, M.; KONG, F.; JANSE, J.H.; MOOIJ, W. M. Hydrological regulation drives regime shifts: evidence from paleolimnology and ecosystem modeling of a large shallow Chinese lake. **Global Change Biology**, Ilinois-USA, v. 23, n. 2, p. 737–754, 2017.

LARA, JL.; LOSADA, I.J.; LIU, P.L.F. Breaking waves over a mild gravel slope: Experimental and numerical analysis. **Journal of Geophysical Research: Oceans**, St. Petersburg-FL, v. 111, n. C11, 2006. DOI 10.1029/2005JC003374.

LIANG, H. & CHEN, X. Capillary-gravity ship wave patterns. **Journal of Hydrodynamics**, Beijing, China, v. 29, n. 5, p. 825–830, 2017.

LIU, M.; SUN, J.; LI, Y.; XIAO, Y. Nitrogen fertilizer enhances growth and nutrient uptake of Medicago sativa inoculated with Glomus tortuosum grown in Cd-contaminated acidic soil. **Chemosphere**, v. 167, p. 204–211, 2017.

MACFARLANE, G.J.; BOSE, N.; DUFFY, J.T. Wave wake: focus on vessel operations within sheltered waterways. **Journal of Ship Production and Design**, EUA, v. 30, n. 3, p. 109–125, 2014.

MIRANDA, I.M.; TOLDO, E.E. JR.; KLEIN, A.H.F.; STRAUSS, D.; VIEIRA DA SILVA, G. The role of cuspate spits on wave attenuation and energy redistribution in a coastal lagoon, Lagoa dos Patos, Brazil. **Geo-Marine Letters**, 2020. https://doi.org/10.1007/s00367-019-00632-9.

NASCIMENTO, B.M. **Desenvolvimento de um método para inibição de incrustação em tubulação de água do mar utilizando ondas ultrassônicas**. Recife, 2019. 76 p. Dissertação (Mestrado), Universidade Católica de Pernambuco.

NETTO, L.G.; GANDOLFO, O.C.B.; MALAGUTTI FILHO, W.; DOURADO, J.C. Integração dos métodos de sísmica de refração de onda se análise multicanal de ondas superficiais (masw) em barragem de terra. In: 16th INTERNATIONAL CONGRESS OF THE BRAZILIAN GEOPHYSICAL SOCIETY. Rio de Janeiro, Brazil. 2019. **Atas**…Rio de Janeiro: Sociedade Brasileira de Geofísica, 2019.

OZKAN, C.; OZKAN, C.; CIGDEM OZKAN. The impacts of wave energy conversion on coastal morphodynamics. **Science of The Total Environment**, Amsterdã-PB, v. 712, p. 136424, 2020.

PAULA, D.L.M.; LIMA, A.C.M.; VINAGRE, M.V.A.; PONTES, A.N.; PAULA, D.L.M.; LIMA, A.C.M.; VINAGRE, M.V.A.; PONTES, A.N. Saneamento nas embarcações fluviais de passageiros na Amazônia: uma análise de risco ao meio ambiente e à saúde por meio da lógica fuzzy. **Engenharia Sanitária e Ambiental**, Rio de Janeiro-RJ, v. 24, n. 2, p. 283–294, 2019.

PEREIRA, M.; TEODORO, A.C.; VELOSO-GOMES, F.; OLIVEIRA, S. Breakwater control system and structural analysis: physical and numerical modelling (Port of Funchal, Madeira Island, Portugal). **Journal of Coastal Conservation**, Alemanha, v. 20, n. 6, p. 455–468, 2016.

PESSIN, J. **Movimentação axial e lateral de dutos com controle de força vertical**. Rio de Janeiro, 120pp. 2017. Dissertação (Mestrado) (Programa de Pós-graduação em Engenharia Civil, COPPE). Universidade Federal do Rio de Janeiro.

PIATAM, I.I.S.E.A. Instituto Piatam. 2020. **Piatam**. Disp. em: https://www.institutopiatam.org.br/. Acesso em: 13 fev. 2020.

PIZZO, N.; DEIKE, L.; MELVILLE, W.K. Lagrangian transport by breaking deep-water surface waves. **AGU Fall Meeting Abstracts**, EUA, v. 31, 2018.

PLAMER, C.B.; LIMA, Y.T.B.; ISOLDI, L.A.; SANTOS, E.D.; ROCHA, L.A.O.; GOMES, M.D.N. Modelagem computacional e método constructal design aplicados a um conversor de energia das ondas do mar do tipo coluna de água oscilante (CAO) analisando a influência em seu desempenho da variação da razão entre o volume de entrada e o volume total da câmara hidropneumática. **Revista Brasileira de Energias Renováveis**, v. 6, n. 3, p.507 – 526. 2017.

RAPAGLIA, J.; ZAGGIA, L.; PARNELL, K.; LORENZETTI, G., VAFEIDIS, A. T. Ship-wake induced sediment remobilization: Effects and proposed management strategies for the Venice Lagoon. **Ocean & Coastal Management**, Amsterdã-UK, v. 110, p. 1–11, 2015.

SAJINKUMAR, K.S.; BINCY, H.S.; BOUALI, E.H.; OOMMEN, T.; VISHNU, C.L.; ANILKUMAR, Y.; THRIVIKRAMJI, K.P.; KEERTHY, S. Picturing beach erosion and deposition trends using PSInSAR: an example from the non-barred southern west coast of India. **Wetlands Ecology and Management**, v. 21, 2020.

TEIXEIRA, H.T. A Avaliação Ambiental Estratégica No Planejamento da Gestão de Recursos Hidricos: Uma Necessidade para o Equilíbrio do Meio Ambiente. **Revista de Direito Ambiental e Socioambientalismo**, v. 2, n. 1, p. 190–209, 2016.

THEMISTOCLES, P.T. **Avaliação Numérico-Experimental de Embarque de Água (Green Water) em FPSO Sujeito a Ondas Oblíquas e de Través**. 2016. Tese – Universidade Federal do Rio de Janeiro, 2016.

ZHU, L.; CHEN, Q.; WANG, H.; CAPURSO, W.; NIEMOCZYNSKI, L.; HU, K.; SNEDDEN, G. Field Observations of Wind Waves in Upper Delaware Bay with Living Shorelines. **Estuaries and Coasts**, Texas-EUA, v. 29 2020.

Submetido em 14 de julho de 2020
Aceito para publicação em 28 de dezembro de 2020